MNK Publication

International Journal of Latest Research in Science and Technology **ISSN (Online):2278-5299**
Volume 4, Issue 2: Page No.46-55, March-April 2015
https://www.mnkpublication.com/journal/ijlrst/index.php

IN VITRO NEW BIOPOLYMER FOR BONE GRAFTING AND BONE CEMENT

Gehan A. Raouf[*1, 2, 3], Hana Gashlan[1], Alaa Khedr[4], Salem Hamedy[5], Hind Al-jabbri[1]
[1]Biochemistry Department, King Abdulaziz University(KAU), Jeddah, K.S.A.,
[2]Medical Biophysics Lab., King Fahd Medical Research Centre, KAU, Jeddah, K.S.A.
[3]Spectroscopy Department, Physics Division, National Research Centre, Cairo-Egypt
[4]Pharmacy Department, KAU, Jeddah, K.S.A.,
[5]Biologys Department, KAU, Jeddah, K.S.A.,

Abstract::- Cements based on synthetic calcium sulfate is among the most investigated material for dental and orthopedic applications in reconstructive surgery. To overcome the short-term cytotoxic effect, brittleness and fast resorption of calcium sulfate dihydrate(CSD), as bone substitute material, CSD was doped with Lepidium sativum water extract(LS) powder and mixed with cow bone mineral (BM) (1: 0.04: 1: wt/wt ratio respectively). The Fourier Transform Infrared (FTIR) spectra of BM-CSD, BM-CSD-LS, and BM-LS composites, compared to BM, were recorded. LS was analyzed by using Gas Chromatography/ Mass Spectroscopy(GC/MS) and Scanning Electron Microscope-Energy Disspersive X-ray(SEM-EDX). The results revealed that the total carbonate/phosphate ratio, type B-carbonate substitution, and acid phosphate content increased dramatically in all tested composites, the maximum increase was detected in BM+CSD+LS composite. Other forms, rather than B-carbonate substitution, takes place such as substitution with Zn, Mg and amino acids. The BM-crystallinity (BMC) decreased significantly in both BM+CSD, B+CSD+LS while, it is slightly decreased in BM+LS composite compared to BMC. Thus, addition of CSD to bone mineral leads to decrease in crystallinity while adding LS only or doping CSD with LS increases the crystallinity of bone mineral compared to BM+CSD composite with increasing in the apatite crystal size and the acid phosphate content as well.

Keywords - Bone Mineral Crystallinity, Bone grafting, Calcium Sulphate Dihydrate, Fourier Transform Infrared Spectroscopy, Gas Chromatography Mass Spectra.

I. INTRODUCTION

Bone is a natural composite material, which by weight contains about 60% mineral, 30% matrix and 10% water [1]. Bone is also a living tissue, with about 15% of its weight being due to the cellular content [2]. The matrix of bone is comprised primarily of type I collagen that is highly aligned, yielding a very anisotropic structure [3].

This organic component of bone is predominantly responsible for its tensile strength. A bone is composed of two main parts, the cortical bone and the trabecular bone. Each presents different mechanical properties and different structures. The cortical bone also is called compact bone whereas the trabecular is sometimes called cancellous or spongy bone [4, 5].

The mineral phase of bone is mainly composed by natural hydroxyapatite (HA). Therefore cements based on synthetic HA and other calcium salts, phosphates and sulfates, are among the most investigated materials for dental and orthopedic applications in reconstructive surgery. Because of their biocompatibility, bone bonding ability, osteoconductivity, nontoxic, and non-inflammatory effects [6, 7]. The principals involved in successful bone grafts include osteoconduction, osteoinduction, and osteogenesis. Osteogenesis only occurs with autografts. The massive bone defects are a great challenge to reconstructive surgery [8]. Therefore, synthetic bone grafts composed of polymers, ceramics or composites, with or without cells and growth factors, have been used for bone regeneration. The ideal bone graft substitute should be biocompatible, bioresorbable, osteogenic, able to provide structural support, easy to use clinically and cost-effective. Calcium sulfate has been used since 1892 as a bone defect filler and is known to be osteoconductive [9, 10]. Calcium sulfate is actually plaster of Paris.

CSD is well tolerated by the tissue, resorbable, acts as a space maintainer that prevents soft tissue from invading the defect until bone can grow on and proved very osteogenic in vivo [11-13]. Over a period of five to seven weeks the calcium sulfate is reabsorbed by a process of dissolution [14]. Calcium sulfate, however, requires a dry environment to set and if it is re-exposed to moisture it tends to soften and fragment. For this reason it has no reliable mechanical properties in vivo and its application should be limited to a contained area. Hence the primary use of calcium sulfates should be as bone void filler [15]. Thus, the disadvantages of calcium sulfate are its transient cytotoxic effect leading to inflammatory reactions, it is completely resorbed following implantation and it has no compressive strength in vivo [16].
This study was conducted as a trail to improve the synthetic calcium sulphate dihydrate based composite as biodegradable bone substitute material in vitro and to tolerate these disadvantages by doping CSD with Lipedium sativum (LS) water extract. Fourier Transform Infrared Spectroscopy (FTIR) was used for the qualitative and quantitative analysis of the new biopolymer. Gas Chromatography mass Spectra(GC/MS), Scanning Electron Microscope-Energy Dispersive X-ray were used to study the chemical and

Publication History
Manuscript Received : *5 April 2015*
Manuscript Accepted : *8 April 2015*
Revision Received : *25 April 2015*
Manuscript Published : *30 April 2015*

morphological constituents of LS. Caw bone mineral (BM) was tested with CSD and LS to form different bone composites The crystallinity of bone minerals, crystal size, type B carbonate substitution, the variation in the carbonate to phosphate ratio and the acid phosphate content among all the composites under investigation were compared and evaluated.

II. MATERIALS AND METHODS

The experimental work of the present study was conducted at the Medical Biophysics Laboratory at King Fahd Medical Research Center, King Abdulaziz University, Jeddah, Kingdom of Saudi Arabia.

Chemicals

All chemicals used in this study were of analytical grade and supplied from different Company for medical & commercial service. Calcium sulfate dihydrate, sodium hydroxide, ether and potassium bromide were purchased from Panreca (Espane) and the ethanol from Fisher Scientific UK limited. Other media were prepared according to the reported methods. The seeds of Lipidium sativum (Family: Cruciferae) were purchased from the local market.

Preparation of lepidium sativum water extract

The seeds were manually cleaned to remove all foreign matter such as dust, dirt, stones, immature and broken seeds. Their colour, length, and shape were examined and the aqueous extract was prepared according to the Moroccan Traditional Phytotherapy [17]. Exactly 1g of powdered seeds was mixed with 100 ml distilled water. The pH of the mixture was measured by pH meter and the pH was 6.21. The mixture was boiled for 10 min, cooled for 15 min, and centrifuged at 3000 rpm for 10 min. The sediment was removed and the supernatant was collected to be used in the experiment. The supernatant was then lyophilized, ground, and sieved to particle sizes 150 μm, 125 μm, and 90 μm. The best of FTIR spectrum for both BM and LS row were obtained with particle size 90 μ.

Bone collection and de-proteination

Fresh femoral cow bones were taken from massacre meat, Jeddah. Calf femoral bones were boiled, both ends were cut, bone marrows were extracted and the bones were cleaned from all soft tissues attached to them. Middle part of the femur was taken and cut into pieces. These pieces were placed in ether for 24 hours, washed, dried in 110°C. Bone pieces were put in NaOH solution 0.5N (2%) using three different temperatures (from 20°C-50°C-80°C).The best bone mineral yield was obtained at 80 °C. After 14 days, bone pieces were washed, dried, ground, and sieved to particle size 90, 125 and 150μm. the best particle size 90 μm has been chosen.

Preparation of Bone Composites

Bone composite groups were prepared by mixing cow bone minerals and medium (water) with both CSD and LS according to Table (1). The liquid medium was prepared with distilled demineralized water. The wetting ratio, i.e. the amount of the medium to be added to the cement, was decided on the basis of workability of the putty formed [16]. The composite was observed to form workable putty only in a narrow range of wetting ratio. Insufficient amount of the medium will make the cement powder an inhomogeneous mass, with which shaping is difficult. Excessive amount of medium, on the other hand, will give a loose paste. For the proposed application, putty that can be shaped with fingers will be ideal [18].

Table 1: The tasted Bone composite groups Composite I Bone and calcium sulfate, Composite II Bone and calcium sulfate and LS, Composite III Bone and LS.

Tasted composites	BM	CSD	LS
Composite I BM+CDS	1g	1g	-
Composite II BM+CDS+LS	**1g**	**1g**	**0.04 ml**
Composite III BM+LS	1g	-	0.04 ml

Infrared Measurement

The FTIR spectra from each composite were obtained in from of KBr peletes by using a Shimadzu FTIR-8400s spectrophotometer with continuous nitrogen purge. For one composite, three IR spectra were obtained from different KBr discs and then co added by using IR-solution software. Typically, 20 scans were signal-averaged for a single spectrum and at spectral resolution of 4 cm^{-1}. Pellets were scanned at room temperature over the range 4000–400 cm^{-1}. Curve fitting to the IR spectra were carried by using Omnic software.

Scanning Electron Microscope–Energy Dispersive X-ray (SEM-EDX)

For SEM studies the samples (LS) were suspended in distilled water, then treated in an ultrasonic bath (BRANSON, 1510) about 20 min. A small drop of this suspension was placed on the double side carbon tape on an Al-Stub and air-dried. All samples were sputtered with a 15 nm thick gold layer (JEOL JFC- 1600 Auto Fine Coater). The specimens were examined with a scanning electron microscope (JSM-6360LA, JEOL, Tokyo, Japan). The microscope was operated at an accelerating voltage of 20 kV. The specimens were analyzed without coating by using Energy Dispersive X-ray unit (EX-23000BU) which was attached to the scanning electron microscope (JSM-6360LA) (JEOL- Tokyo- Japan). Quantitative method ZAF and characterization method as pure.

Gas Chromatography-Mass spectrometry

A gas chromatograph GC–mass spectrometer (MS) Clarus 500 GC/MS (PerkinElmer, Shelton, CT) was used. The software controller/integrator was Turbo Mass, version 4.5.0.007 (PerkinElmer). An Elite 5MS GC capillary column (30 × 0.25-mm × 0.5 μm, PerkinElmer) was used. The carrier gas was helium (purity 99.9999%) at a flow rate of 0.9 mL/min (32 p.s.i., flow initial 40 cm/s, split; 1:40). Temperature conditions were: inlet line temperature, 270°C; source temperature, 210°C; trap emission, 100v; and electron energy, 70 eV. The column temperature program was: 50°C for 5 min, increased to 220 °C (rate, 15°C/min), and held for 5 min. The injector temperature was 260°C. MS scan was from 50 to 350 m/z. Screw-capped borosilicon mini-reaction

vials 2-mL (v-shaped, with TFE liners) were used for stress testing (Alltech, GmbH, Unterhaching, Germany).

Derivatization for GC/MS analysis

Exactly 1 mg dried sample extract (aqueous extract of LS) was transferred to 2-mL borosilicon reaction vial and dissolved in acetonitrile (50 µL). A volume of 50 µL of N-methyl-N-trimethylsilyl-trifluoroacetamide (MSTFA) was added, mixed and the vial screw capped and left at 80 °C for 10 min. The vial was cooled and the content was transferred to a total recovery vial (1 mL) and a volume of 1 µL was injected for GC/MS analysis. The generated data was explored for the excising compounds using NIST2008 database.

Table 1: The tasted Bone composite groups Composite I Bone and calcium sulfate, Composite II Bone and calcium sulfate and LS, Composite III Bone and LS.

Statistical Analysis

Different absorbance ratios for specific bands were calculated and plotted for each composite. For the analysis of variance the (Kruskal-Wallis) test was conducted to confirm the results obtained from IR measurements. The Mann-Whitney test was applied to investigate the significance of the difference between composites.

Using Ward's algorithm Euclidean distance linkage tree, Hierarchical cluster analysis (HCA) was used to classify the second derivative of the FTIR spectra and to determine if there is structural difference among the tested composites and the BM [19]. HCA depends on the similarity between two objects [20] and was performed by PAST version 2.17b software.

III. RESULTS

FTIR measurements

The FTIR spectra of cow BM, CSD, LS, were obtained and are shown in Fig (1). All spectra were normalized and base line corrected. The characteristic IR bands of bone minerals together with their band assignments were given in Table (2) according to the literatures.

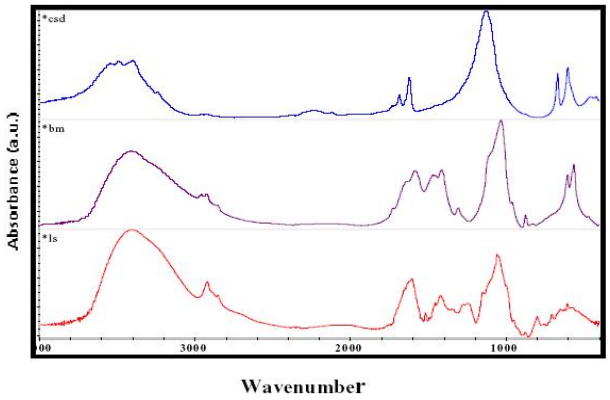

Fig. 1. Overlaid FTIR spectra of row materials BM, CSD, and LS over the range4000-400cm^{-1}.

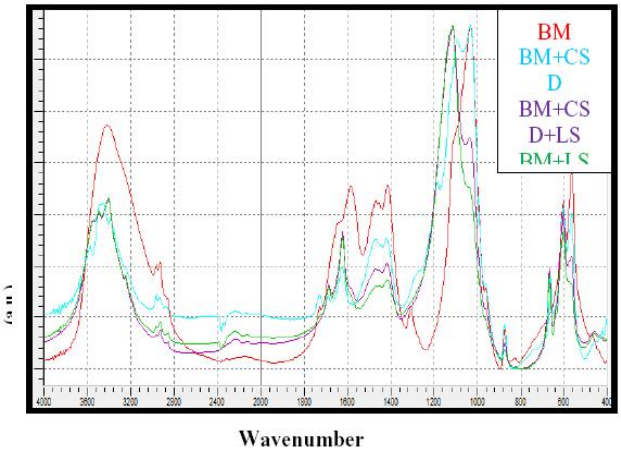

Fig. 2. Overlaid FTIR spectra of cow bone mineral (BM), BM+ calcium sulphate dehydrate (CSD), BM+CSD+ Lepidium sativum water extract (LS), and BM+LS composites over the range (4000-400 cm^{-1}).

The phosphate bands centered around 960,1030 cm^{-1} arise primarily from symmetric and antisymmetric PO_4^{-3} stretching modes of the amorphous calcium phosphate respectively [21]. The band of PO_4^{-3} antisymmetric bending 500-700 cm^{-1} in bone mineral, resolved into two distinct peaks at 604, 567 cm^{-1}, characteristic of well crystallized apatite phase [22].

IR spectral signature of bone mineral composites

The FTIR spectra of the tested composites together with BM spectrum were overlaid and illustrated in (Fig 2).

Composite 1 (BM+CSD)

Careful inspection of the raw FTIR spectra of BM compared to BM+CSD revealed the following:

1- Decrease in the intensity of the phosphate band around 565 cm^{-1} with appearance of week broad shoulder around 576 cm^{-1} (HA).
2- Reduction in the intensity of the phosphate band around 603 cm^{-1}.
3- Appearance of a new sulphate bands around 1625 and 663 cm^{-1} .
4- A slight increase in the intensities of the small bands around 960, 873 cm^{-1} corresponds to phosphate and carbonate groups respectively.
5- There are dramatic changes in the region 960-1350 cm^{-1} include the appearance of new broad band around 1092 cm^{-1}, well defined band around 1122 cm^{-1} and appearance of new band around 1182 cm^{-1}.
6- A decrease in the intensity of the carbonate band in the range 1400-1500 cm^{-1}.

v: stretching vibrations, δ: bending vibrations, s: symmetric, as: asymmetric (Nikolaos and Margaret 2010; Nyquist et al., 1997).

Composite 2 (BM+CSD+LS)

Doping Bone+CSD with LS leads to:

1- More reduction in the phosphate band around 564 cm^{-1}, the week shoulder appeared at 575cm^{-1} splits into ill resolved band around 577cm^{-1}.
2- More reduction in the intensity of the phosphate band around 600 cm^{-1}.

3- Appearance of a strong shoulder around 640 cm^{-1} together with increase in intensity and broadening of the new band appeared earlier around 662 cm^{-1} which now shifted to 667 cm^{-1}.
4- Instead of the slight increase in the intensities of the small bands around 960, 873 cm^{-1} a dramatic reduction in these intensities are observed after adding LS to the cement.
5- Severe reduction in the phosphate band around 1030 cm^{-1} together with the transfer of the broad strong shoulder at 1114 cm^{-1} into a very strong broad band.
6- Doping CSD with LS to the caw bone leads also to further reduction in the carbonate bands in the range 1400-1500 cm^{-1}.
7- Increase in the intensity of the new broad sulphate bands around1625 cm^{-1}and1686cm^{-1}.

Composite 3 (BM+LS)

Addition of LS to the Bone minerals leads to the following changes in IR spectrum as follows:

1- Severe reduction in the phosphate band around 562 cm^{-1} the band now appeared as a strong shoulder. There is a decrease in the intensity of the other phosphate band around 603 cm^{-1} with the appearance of new shoulder at 616 cm-1, ill resolved band around 638 cm^{-1} and a will defined medium band around 667 cm^{-1}.
2- Disappearance of the small band around 825 cm^{-1}, reduction in the band intensity around 873 cm^{-1} and the weak band around 960 cm^{-1} transferred into a weak shoulder too.
3- Dramatic reduction in the band around 1030 $cm^{-1}$with the remarkable increase in the band intensity and area of the band at 1113 cm^{-1}as well.
4- Disappearance of the small band at 1305 cm^{-1}together with a marked decrease in the carbonate bands over the range 1400-1500 cm^{-1}.
5- Increase in the intensity on the of new broad sulphate bands around 1625 $cm^{-1}$and 1686 cm^{-1} .

Curve fitting analysis

To elucidate the phosphate and carbonate band positions and quantitate their relative contributions, second derivative spectroscopy and then curve fitting to the phosphate region (900-1200 cm^{-1}) and carbonate band (850-900 cm^{-1}) region were carried(Fig. 3) .The peak intensity, HBW and area are listed in Table (3). The curve fitting of the carbonate band near 875 cm^{-1}, known to be resolved into at least three underlying sub-bands corresponding to A-type CO_3^{-2} at 878 cm^{-1}, B-type CO_3^{-2} at 871 cm^{-1}, and relatively minor nonspecific or surface CO_3^{-2} at 866 cm^{-1} but in case of cow bone minerals the peak resolved bands reveled only the presence of B type carbonate around 874 cm^{-1}, no evidence of presence of A type carbonate band. It is clear from the table that the area of B type carbonate substitution decreased first In all tested composites B+CSD > B+CSD+LS > B+LS in order from 2.422 to 2.240 1.276, 1.024 respectively.

Table 2: Proposed band assignments of the FTIR spectra of bone mineral in the 4000-400cm^{-1} spectral range.

Wave number (cm^{-1})	Band assignment
3572	OH^- ν vibration modes
1685 1620	OH^- ν vibration modes
1400 1500	ν and as mode of vibration ion CO_3^{-2}
1012	PO_4^{-3} as ν phosphate
960 1030	s and as PO_4^{-3} stretching mode of amorphous calcium phosphate.
871	CO_3^{-2} carbonate δ
856	CO_3^{-2} as carbonate δ
630	OH^- ν vibration modes
600	PO_4^{-3} δ (mineral)
557	PO_4^{-3} δ (mineral)
561,604	as ν PO_4^{-3} characteristic of well crystallized apatite phase
473	PO_4^{-3}

Table 3: Bands position, intensity, HBW, and area of the carbonate and phosphate sub-bands.

Groups	Wave number cm^{-1}	Intensity	HBW	Area
BM	874.027	0.115	16.067	2.4222
	957.238	0.133	31.834	5.6913
	1014.234	0.403	44.131	23.4672
	1033.611	0.543	47.008	33.645
	1060.130	0.365	47.011	22.589
	1115.092	0.248	37.232	11.992
BM+CSD	872.72	0.091	18.148	2.240
	952.628	0.090	59.661	7.533
	1021.570	0.357	57.022	28.504
	1040.926	0.198	58.572	16.309
	1060.651	0.131	58.683	10.797
	1112.127	0.469	58.162	38.332
BM+CSD +LS	871.98	0.053	18.693	1.025
	953.300	0.081	53.477	6.076
	1026.272	0.307	52.471	22.628
	1043.211	0.060	52.888	4.456
	1060.384	0.142	52.977	10.567
	1109.674	0.507	52.720	37.485
BM+LS	872.013	0.046	16.935	1.025
	957.189	0.057	26.410	1.999
	1020.670	0.2366	27.749	8.747
	1036.469	0.2456	28.296	9.257
	1054.300	0.2084	28.130	7.811
	1071.708	0.2242	28.347	8.4708
	1118.759	0.2378	28.774	9.1245

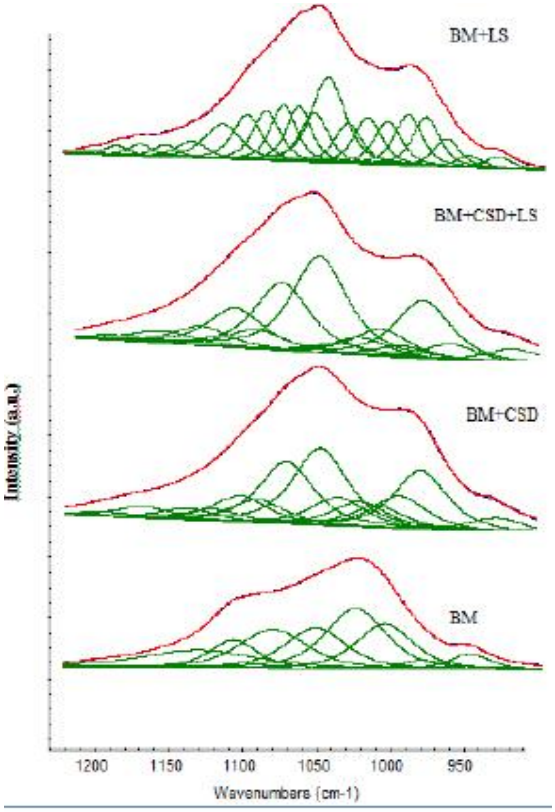

Fig. 3. Curve fitting analysis of BM, BM+CSD, BM+CSD+LS, BM+LS composites in the IR spectral range 1200-950 cm^{-1}.

Clustering analysis

The dendrograms of HCA created two initial clusters represented by two branch, which were further subdivided into smaller clusters (Fig. 4). Wards method Euclidean distances dendrogram, linkage tree, succeeded to distinguish between all tested composites compared to the BM but the distance are small except that of sample B of composite I. However, it failed to distinguish between LS treated groups (composite II & III) and BM+CSD (composite I).

Ratio measurements

From the FTIR row spectra:

1- The carbonate to phosphate ratio [(871cm^{-1})/ (1030+960cm^{-1})] CO_3^{2-}/PO_4^{3-} was deduced from the ratio of the integrated areas of respective raw spectra.

From the curve fitting analysis:

The area ratios measured (the area values were taken from Table (3) are

2- 1060/1020 cm^{-1} which indicates the bone mineral crysatallinty

3- 1112/960 cm^{-1} which indicates the acid phosphate content

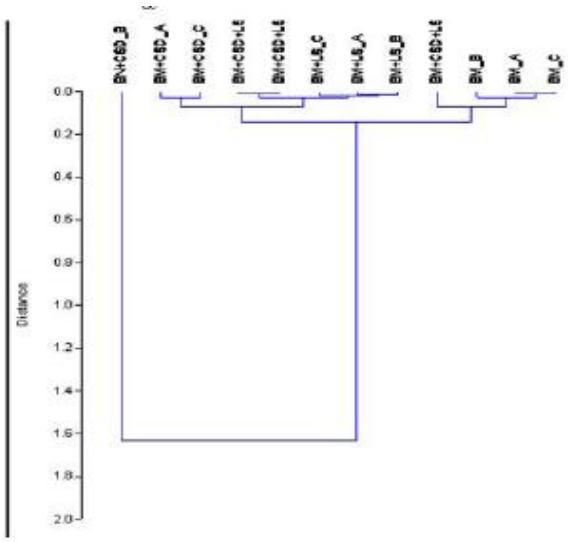

Fig. 4. HCA spectral analysis of carbonate and phosphate region (1600-400 cm^{-1}); obtained from caw bone mineral (BM) and the BM+CSD, BM+CSD+LS and BM+LS composites (each group include 3 different samples).

These ratios were calculated and listed in Table (4).

The total carbonate/phosphate ratio increased dramatically in all bone composites under investigation the maximum increase was detected in B+CSD+LS. The mineral crystal linty decreased significantly in both B+CSD, B+CSD+LS while, it is slightly decreased in B +LS composite compared to bone mineral crystallinty. On the other hand, the acid phosphate content was increased dramatically among all bone composites under investigation. The maximum value was recorded in composite B+CSD+LS.

Table 4: The variation of carbonate/phosphate, mineral crystallinity, and the acid phosphate ratios among the tasted composites compared to bone mineral.

Parameter / Groups	BM (a)	BM+CSD (b)	BM+CSD+LS (c)	BM+LS (d)
From row spectra area of carbonate(855-890cm^{-1})/phospate(1030+960cm^{-1})	.0154±.007^{bc}	.0352±.006^{acd}	.0668±.0097^{abd}	.0274±.0075^{bc}
Mineral crystallinity from(Curve fitting) 1060 cm^{-1}/1020 cm^{-1}	0.9624±.032^{bc}	.3787±.054^{acd}	0.4669±.089^{abd}	0.8930+.035^{bc}
Acid phosphate from(Curve fitting) 1112cm^{-1}/960 cm^{-1}	2.107±.071^{bcd}	5.089±.081^{acd}	6.170±.054^{abd}	4.567±.09^{abd}

Values are means±S.D. Significance at $p < 0.05$. Letters indicate significance; a=significant against the control (BM), b= significant

against BM+CSD, c= significant against BM+CSD+LS, d= significant against the BM+LS

GC/MS of Lepidium sativum water extract

The different chemical components in LS water extract were analyzed by using GC/MS. The results revealed that LS is rich in many important compounds such as a) sinapic acid, b) silane, c) sabinene, d) butanoic acid, e) leucine f) squalene, g) aspartic acid, the most important compounds in the LS water extract, the chemical structure and the most beneficial uses in medicine, especially in case of bone repair, are given in Table S1. The detected compounds were identified by matching the NIST2008 Database as intact compound or trimethyl-silyl derivative. The compounds containing the –OH or NH functional groups were detected as –O-TMS or –N-TMS derivatives (volatile). The TMS derivatized compounds were more characterized by the fragment m/z 73 corresponds to O-TMS or N-TMS moiety.

The MS spectrum of sinapic acid (Table S1) was characterized by the major abundant m/z peaks at 164 (100%) and 179 (30%), which are due to cleavage of –COOH and O-CH_3 groups. Sabinene, squalene, and leucine were confirmed by 95% match with a corresponding database. Leucine, aspartic acid, and butanoic acid were detected as their O-TMS derivative. (Fig. S1) shows the analysis results for LS.

SEM –EDX

The surface morphology, and the abundant elements found in LS water extract were examined by SEM. (Fig. 5) shows that LS possesses flat sheets that correspond to the presence of calcium phosphate mineral resembling that found in the apatite mineral in bone, and the presence of both aspartic acid and sulfonamide crystals. (Fig. 6) shows the EDX patterns corresponding to SEM micrograph. A considerable amount of boron, carbon, oxygen, sodium, magnesium, aluminum, phosphate, iron, silver, potassium, calcium, and sulfur ions were clearly recognized in the EDX of the LS water extract. Little amounts of cadmium, manganese and zinc were also detected.

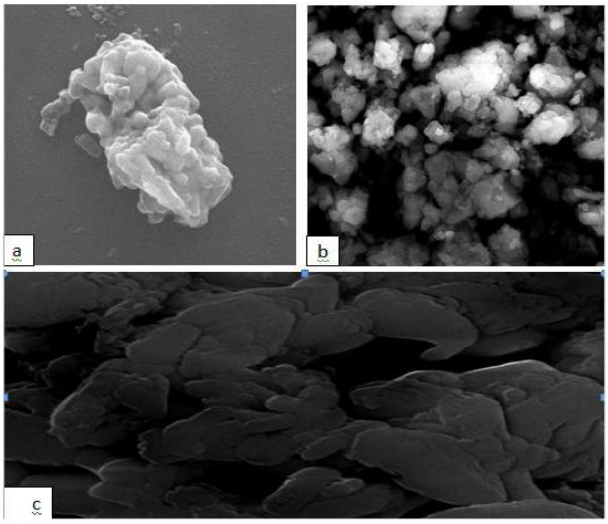

Fig. 5. The surface morphology of *lepidium satvium* water extract (a): sulfonamide crystals, (b): aspartic acid, (c); calcium phosphate examined by SEM-micrograph.

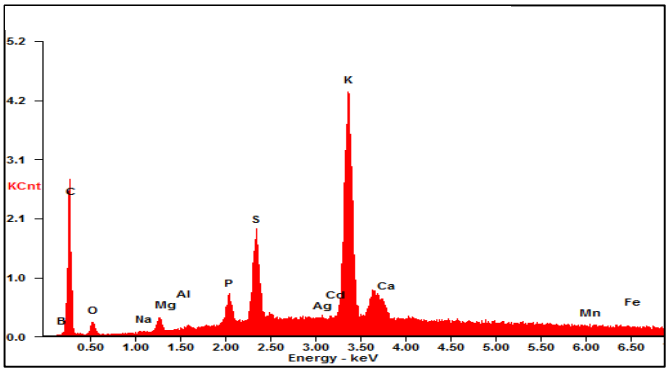

Fig. 6. The EDX patterns show the abundant elements found in the LS water extract examined by SEM-EDX.

IV. Discussion

Replacement of extensive local bone loss is a significant clinical challenge. There are a variety of techniques available to the surgeon to manage this problem, each with their own advantages and disadvantages. It is well known that there is morbidity associated with harvesting of an autogenous bone graft and there are limitations in the quantity of bone available. Alternatively allografts have been reported to have a significant incidence of postoperative infection and fracture as well as the potential risk of disease transmission [23, 24]. During the past 30 years a variety of synthetic bone graft substitutes has been developed with the aim to minimize these complications. The benefits of synthetic grafts include availability, sterility and reduced morbidity [25, 26]. of the numerous shortcomings of biologic graft, many research efforts in the bone regeneration field deal with the development of bone graft substitutes and their employment in tissue engineering [27, 28].

Injectable, in situ polymerizable, biodegradable scaffold that can guide bone regeneration while providing structural support to the region will alleviate many of the problems encountered with current treatment methods [29].

As reported, gypsum (CSD), in contact with body fluids, forms calcium phosphate deposits which are responsible for conducting and accelerating bone formation [12, 30, 31]. It is well tolerated by the tissue, resorbable, acts as a space maintainer that prevents soft tissue from invading the defect until bone can grow on and proved very osteogenic in vivo [11-13]. Normal and diseased bone mineral has been extensively studied with IR spectroscopy [32, 33]. FTIR has been used to investigate HA in both model systems and calcified tissues [34]. One of the advantages of this method lies in the fact that FTIR spectra provide information from all tissue components. The protein and mineral constituents produce intense, structure sensitive IR bands. Part stoichiometric HA, $Ca_{10}(PO_4)_6(OH)_2$ in its most common form, occurs as a hexagonally packed crystal. Apatite from biological tissues is carbonate substituted ~5-6% by weight [35]. The CO_3^{-2} ion can substitute for either phosphate ions (PO^{-3}_4) type B carbonate, the major substitution site in bone and dentin [36] or for hydroxyl ions (OH^-) type A carbonate, which occurs at a significant level in dental enamel [35], of

HA, leading to a nonstiochiometric apatite mineral [37, 38, 39a,b]. In addition to these insertion sites, a labile carbonate species was identified and is thought to represent surface carbonate [33].

Other possible substitutions include replacement of the hydroxyl group by fluoride ion [21]. The crystallinity, i.e. the HA crystal size and perfection, of apatites are of great biomedical interest, because smaller, more imperfect crystals, being subject to dissolution, may affect the extent of bone loss in osteoporosis and other metabolic bone disease [40]. Traditionally, X-ray diffraction is the technique of choice for determination of apatite crystal size. In contrast, structural information relating to the apatite mineral in macroscopic, as well as microscopic samples can be readily obtained from IR spectroscopy [21].

Accordingly, the result obtained from this study will be focused on the HA crystal size, bone mineral crystallinity, the degree of B carbonate substitution and the acid phosphate content among the tested composites (BM, BM+CSD, BM+CSD+LS, BM+LS) compared to bone minerals.

Bone Mineral Cross linking with CSD and/or LS

It is well known that the disappearance and the appearance of new absorption bands, the change in band intensity as well as observed band shifts are evidences for cross linking. Otherwise, the bone mineral plus the added cement and/or LS would appear as a combination of all tested sample in one spectrum.

Bone Mineral Crystal Size and Crystallinity

When the symmetry in the HA crystal is lowered, the symmetric stretch of PO_4^{-3} assigned to amorphous calcium phosphate appears as a weak band in the bone spectrum between 950-970 cm^{-1} [21]. The phosphate bands are known to increase in intensity as mineral crystallinity/perfection is enhanced [21].

As mentioned before, the peaks at 604-567 cm^{-1} indicate the well crystallized apatite phase [22]. The peak at 567 cm^{-1} decreased dramatically in all tested composites compared to the slight observed decrease in the band intensity of 604 cm^{-1} band. The maximum reduction in the PO_4^{-3} 567 cm^{-1} band intensity was observed in BM+LS composite. The decrease in the intensity of this band may be attributed to the increase in the apatite crystal size rather than an expected increase in the apatite crystallinity.

It was proved earlier that the decrease in the intensity and band area of the ~1060 cm^{-1} band means the increase in the crystal size of the apatite [21]. The relative area of the sub-bands at 1060 cm^{-1} [41] or the ratio area of the 1030 and 1020 cm^{-1} sub-bands [42] correlate linearly with the HA crystal size and perfection in the c-axis direction as determined by X-ray diffraction analysis [43]. The area of the band at ~1060 cm^{-1} decreased significantly from 22.6 in bone mineral to 10.8, 10.6 and 7.8 in the BM+CSD, BM+CSD+LS and BM+LS composites, respectively.

It is known also that the shift of the band at ~1027 cm^{-1} towards higher freq uency is an indicative of increasing apatite crystal size. Nancy et al.,1991 found that the frequency is not than 1027 cm^{-1} for apatite crystal size less than ~160A^o, and increases to 1028-1032 cm^{-1} for crystal sizes between ~160-190A^o. They also reported that well crystallized apatites ~200-450A^o revealed additional spectral features compared to the more poorly crystalline materials; the higher the crystallinity the higher increased number of band obtained from curve fitting [21].

These results agree with the results obtained from the curve fitting analysis. The maximum number of sub-bands was obtained from BM+LS composite which has the larger crystal size, as mentioned before. On the other hand, the band shift to higher wave number from 1014.23 in bone apatite to 1021.57, 1026.27 and (1020.67+1036.46) in BM+CSD, BM+CSD+LS and BM+LS composites, respectively strongly support the above mentioned results. Compared to bone mineral, the crystallinity ratios of all tested composites were a decreased from 0.962 in bone mineral to 0.379, 0.467 and 0.893, in BM+CSD, BM+CSD+LS and BM+LS composites, respectively. These decreases in BMC were accompanied by decrease in FTIR band intensity of phosphate band too. Except in the composite BM+CSD, the observed slight increase in the intensity of the band at 960 cm^{-1}, which represents the amorphous PO_4^{-3}, may be attributed to the formation of HA when CSD is mixed with the bone mineral (in the presence of water), as mentioned earlier. Gypsum (CSD), in contact with body fluids, forms calcium phosphate deposits which are finally responsible for conducting and accelerating bone formation [12, 30, 31].

The SEM results also indicated the presence of calcium phosphate plates resembling those found in bone apatite.

While, the observed reduction in the 1030,960 cm^{-1} represents the amorphous PO_4^{-3}after adding LS to the former composite, this may be explained by the crystallinity as well as the crystal size of HA in composite BM+CSD+LS are higher than composite BM+CSD, although they are both much lower than that of bone mineral, as described earlier.

These results also agree with Nancy et al., 1991 results. They indicated that incorporation of the amino acids, which occurs through a specific interaction with the HA structure, affects the degree of crystallinity of the apatite phase. The composites are able to support the growth of MG63 cells in vitro and promote their differentiation. The presence of the acidic amino acids allows controlling the crystal dimensions and favors' osteoblasts proliferation, activation of their metabolism and differentiation, which is of high importance for potential biomedical applications. In vitro studies [44 indicated that ASP can act as a nucleating agent for apatite and influence its further growth.

LS water extract as revealed from GC/MS contains aspartic acid and leucine and they both may play a vital role in controlling the HA crystal size and crystallinity. Thus, addition of CSD to bone mineral leads to a decrease in crystallinity while adding LS only or doping CSD with LS increases the crystallinity of bone mineral apatite compared to BM+CSD composite alone with increasing in the apatite crystal size.

Type B Carbonate Substitution & Carbonate to Phosphate Ratio

The carbonate to phosphate ratio indicates the extent of carbonate incorporation in the hydroxyapatite lattice, and the curve-fitting of carbonate bands reveals whether the

carbonate has replaced hydroxide (A-type) or phosphate (B-type) in the apatite lattice [43]. The increase in B type carbonate band at 873 cm^{-1} in the case of BM+CSD composite is evidence of substitution. This result was evident by the increase in carbonate to phosphate ratio calculated from IR area ratios and Raman intensity ratios as well. Moreover, a decrease in carbonate band over the range 1400-1500 cm^{-1} are attributed to the changes in carbonate type during forming the composite. By contrast, the increase in carbonate to phosphate ratio in LS composites (BM+CSD+LS and BM+LS) cannot be considered as an increase in B-carbonate substitution only. This ratio may also increase when phosphate content decreases. LS, as analyzed by GC/MS, has different ions for substitution in addition to carbonates such as Zn and Mg. It was mentioned earlier that there was a significant decrease in the intensities of 1030 cm^{-1} and 960 cm^{-1} phosphate bands in non-Stoichiometric HA. The band at 1045 cm^{-1} reflect the amount of B-type CO_3^{-2} [36]. This band area, which appeared in the curve fitting analysis in BM+CSD, BM+CSD+LS and BM+LS composites, decreases from 16.31 to 4.46, and 9.26, respectively. This supports the above discussed results. Only The BM+CSD composite leads to an increase in type B carbonate substitution with also increase in amorphous phosphate due to the transfer part of CSD to form calcium phosphate deposits [12, 30, 31] while in LS composites another substitution takes place.

Carbonation of mineral tends to increase in normal bone as the mineral matures [45]. Thus, doping of CSD with LS water extract limits the degree of type B-carbonate substitution.

Acid Phosphate Content

As mentioned earlier, incorporation of cortical grafts is initiated by osteoclasts rather than osteoblasts. The acidic environment is essential for bone resorption [46]. These explain the increase in acid phosphate content in all tested composites and the maximum value was recorded for BM+CSD+LS composite (6.169) which is considered as an advantage of this composite compared to the others. The mineral content of bone is mostly hydroxyapatite with small amounts of carbonate, magnesium and acid phosphate [47]. This acid phosphate stimulates bone remodeling in the same way it stimulates osteoclast to start resorption.
Leucine is an anticatabolic agent that promots healing of broken bones [48.

Squaline and Zn ions inhibit bone resorption and stimulate osteoblast for bone formation. It has been shown that Zn acts to increase bone formation and mineralization, decrease bone resorption and stimulate alkaline phosphatase (ALP) activity, in both calvaral organ cultures and osteoblast cell cultures [49-51].

Saeed et al. (2009)[52] investigated the influence of Zn ions incorporated into calcium sulfate ceramics on the physical, physicochemical, and biological properties of the material as an important bone substitute. The zinc ions have been reported to increase the alkaline phosphatase (ALP) activity and DNA content of the bone cells, leading to acceleration of osteogenesis of osteoblasts [53].

The cellular mechanism of zinc action in osteoblastic cells has not been fully clarified. Zinc demonstrated stimulating cell proliferation and differentiation, as well as protein synthesis in osteoblatic cells [54, 55]. Once bone matrix synthesis begins in osteoblast culture models, such as osteoblastic MC3T3-E1 cells, the cells differentiate in accordance with the gene activation and protein synthesis of osteoblast markers. Alkaline phosphatase (ALP) is one of the most representative bone marker proteins for osteoblast differentiation [56,57].

Bone growth and remodelling are normal physiological events that occur at a high rate throughout childhood and adolescence, and to a much lesser extent during adult years. It is the net result of the activity of two types of bone cells which have opposing actions: those that synthesise new bone material, mainly, osteoblasts, and cells called osteoclasts, which are responsible for resorbing or breaking down existing bone material [58].

Thus, this unique balance between matters that stimulate bone resorption and that stimulate bone formation makes the composite BM+CSD+LS the optimum composite can be used in bone grafting. The LS water extract also contains squalene which can be used as an antidote to reduce drug toxicity [59]. Sabinene has pronounced anti-inflammatory and antibacterial properties, it could be used as an additional therapy, together with the antibiotics in order to increase their efficiency [60]. Sinapic acid has stimulatory effects on bone formation and inhibitory effects on bone resorption in tissue culture in vitro [61]. Silane showed excellent osteoconductivity and strong enough mechanical properties for clinical use [62].

V. CONCLUSIONS

Calcium sulfate compounds are becoming of increasingly great importance in the field of biomaterials. Doping CSD with LS leads proves other types of bone substitution rather than type B carbonate, due to the presence of other ions such as Zn, Mg and amino acids such as aspartic acid in LS water extract, and control the hydroxyapatie crystal size. The increased acid phosphate content (maximum value was detected in composite BM+CSD+LS) is considered now as a great advantage of these composite; this acid phosphate stimulates bone remodeling in a way it stimulates osteoclast to start resorption. Moreover, the presence of zinc ions acts to increase bone formation, mineralization and decreases bone resorption. It recommended that if tested in vivo the BM+CSD+LS composite would be a very promising bone substitute materials, which could be osteogenesis and has also a remarkable anti-inflammatory, antifungal and antibacterial effects.

ACKNOWLEDGMENT

This work was supported by King Abdul Aziz City for Science and Technology, grant number A-S-11-0709.

REFERENCES

[1] ATHANASIOU, K. A., C. F. ZHU, D. R. LANCTOT, C. M. AGRAWAL, ANDX. WANG. 2000. FUNDAMENTALS OF BIOMECHANICS IN TISSUE ENGINEERING OF BONE. TISSUE ENGINEERING. 6, 361-381.

[2] Lodish, H. 1995. Molecular Cell Biology Scientific American Books. New York.

[3] Demirkiran, H. 2012. Bioceramics for osteogenesis, molecular and cellular advances. Adv Exp Med Biol. 760, 134-47.

[4] Meunier, P. J., and J. F. Brantus. 1999. Losteoporose Le quotidien du medecin.

[5] Weiner, S., W. Traub.1992. Bone structure: from angstroms to microns. Faseb. 6, 879-885.

[6] de Groot, K. 1983. Ceramic of calcium phosphate: Preparation and properties; CRC Press Inc.

[7] Bajpai, P. K. 1992. A novel device for sustained long term delivery of drugs. Bioceramics 3, 87–89.

[8] Herve, P., V. Veronique, B. Wassila, M. Alain, de P. Cindy, B. Marianne, O. Karim, S. Laurent, and G. Genevieve. 2000. Tissue-engineered bone regeneration. Nature Biotechnology. 18, 959–963.

[9] Greenwald, A. S., S. D. Boden, V. M. Goldberg, Y. Khan, C. T. Laurencin, and R. N. Rosier, The Committee on Biological Implants.Bone-graft substitutes: facts, fictions, and applications. J.Bone Joint Surg Am. 83, 98-103.

[10] Kelly, C. M., R. M Wilkins, S. Gitelis, C. Hartjen, J. T. Watson, and P. T. Kim. 2001. The use of a surgical grade calcium sulfate as a bone graft substitute: results of a multicenter trial. Clin Orthop 382, 42-50.

[11] Pecora, G., D. De Leonardis, and J. Ricci. 2001. L'uso del solfato di Calcio Nelle Tecniche Rigenerative Multidisciplinari. Edizioni Elite Service, 13–77.

[12] Murashima, Y., G.Yoshikawa, R. Wadachi, N. Sawada, and H. Suda. 2002. Calcium sulphate as a bone substitute for various osseous defects in conjunction with apicectomy. Int. Endod 35, 768.

[13] Strocchi, R., G. Orsini, A. Iezzi, C. Scarano, G. Rubini, A. Pecora, and J. Piattelli. 2002. Bone regeneration with calcium sulfate: evidence for increased angiogenesis in rabbits. Oral Implantology 18, 273.

[14] Bell, W. H. 1964. Resorption rates of bone and bone substitutes. Oral Surg. 17, 650–7.

[15] Coetzee, A. S.1980. Regeneration of bone in the presence of calcium sulphate. Arch. Otolaryngol. 106, 405–9.

[16] Goren, S, H. Gokbayrak, and S. Altintas. 2004. Production of hydroxylapatite from animal bone. KEY ENGINEERING MATERIALS, 264-268: 1949-1952.

[17] Eddouks, M., M. Maghrani, N. A Zeggwagh, and J.B. Michel. 2005. Study of the hypoglycaemic activity of lepidium sativum l. Aqueous extract in normal and diabetic rats. J. Ethano. Pharmacol 97, 391–395.

[18] Bull, M., K. Manoj, H. K. Varma, and R. Sivakumar. 2000. On the development of an apatitic calcium phosphate bone cement. Biomedical Technology Wing. 23, 135–140.

[19] Forina, M., C. Armanino, and V. Raggio. 2002. Clustering with dendrograms on interpretation variables. Analytica Chimica Acta 454: 13-19.

[20] Abeysekara, S., D. Damiran, and P. Yu. 2013. Spectrochimica Acta - Part A: Molecular and Biomolecular Spectroscopy.102, 432-442.

[21] Nancy, P., B. Adele, and M. Richard. 1991. Novel infrared spectroscopic method for the determination of crystallinity of hydroxyapatite minerals. Biophysical Society. 786-793.793.

[22] Gunasekaran, K. and S.Thotapallip. 2011. Preparation and characterization of a novel bone graft composite containing bone ash and egg shell powder. Indian Academy of Sciences. 34, 177-181.

[23] Su-Gwam, K., K. Hak-Kyun, and L. Sung-Chul. 2001. Combined implantation of particulate dentine, plaster of Paris, and a bone xenograft (Bio-Oss1) for bone regeneration in rats. CranioMaxillofac Surg Clin North Am 29, 282–288.

[24] Navarro, M., S. del Valle, S. Martinez, S. Zeppetelli, L. Ambrosio, J. A Planell, and M. P. Ginebra. 2004. New macroporous calcium phosphate glass ceramic for guided bone regeneration. Biomaterialsn 25, 4233–4241.

[25] Thomson, R., M. J. P., Yaszemsk, J.M. owers, and A.G. Mikos. 1994. Fabrication of biodegradable polymer scaffolds to engineer trabecular bone. Biomater Sci Polym.7, 23–38.

[26] Giovanna, G., D. Alfredo, L. Paola, and M, Mario. 2007. Development of a new calcium sulphate-based composite using alginate and chemically modified chitosan for bone regeneration. Wiley Inter Science 34.

[27] Damien, C. J. and J. R. Parsons. 1991. Bone grafts and bone graft substitutes: A review of current technology and applications. Appl Biomater 2, 187–208.

[28] Ilan, D. I. and A. L. Ladd. 2003. Bone graft substitutes. Operat Tech Plast Reconstr Surg 9, 151–160.

[29] James, D. K., Y. Simon, K. Leda, W. Mark, and G. M. Antonios. 2009. Injectable Biomaterials for Regenerating Complex Craniofacial Tissues. Adv Mater 21, 3368–3393.

[30] Ricci, J. L., H. Alexander, P. Nadkarni, M. Hawkins, J.Turner, S. Rosenblum, L. Brezenoff, D. De Leonardis, and G. Pecora. 2001. Biological Mechanisms of Calcium Sulfate Replacement by Bone. Bone engineering. 332.

[31] Carinci, F., A. Piattelli, G. Stabellini, A. Palmieri, L. Scapoli, G. Laino, S. Caputi, and F. Pezzetti. 2004. Calcium sulfate: Analysis of MG63 osteoblast-like cell response by means of a microarray technology. Biomedical Materials Research 71B, 260.

[32] Walters, M. A., Y.C. Leung, N. C. Blumenthal, R. Z LeGeros, and K. AKonsker. 1990. A raman and infrared spectroscopic investigation of biological hydroxyapatite. Inorg Biochem 39, 193–200.

[33] Rey, C., B. Collins, T. Goehl, I. R. Dickson, and M. J. Glimcher. 1989. The carbonate environment in bone mineral: A resolutionenhanced Fourier transform infrared spectroscopy study. Calcif Tissue Int 45, 157–164.

[34] Bailey, R. T. and C. Holt. 1989. Fourier transform infrared spectroscopy and characterization of biological calcium phosphates. Macmillan Press. London.

[35] Legeros, R. Z. 1981. Apatites in Biological Systems. Prog. Crystal. Growth Charact. 4, 1-45.

[36] Yang, E. P., W. E. PASCHALIS, A.L. MAYO, A. Boskey, and R. Mendelsohn. 2001. Infrared Microscopic Imaging of Bone: Spatial Distribution of CO_3. Bone and Mineral Research. 16.

[37] Elliott, J. C.1962. The infrared spectrum of the carbonate ion in carbonate-containing apatites. Dent Res 30, 1284.

[38] Emerson, W. H, and E. E. Fischer. 1962 The infra-red absorption spectra of carbonate in calcified tissues. Arch Oral Biol. 7, 671-683.

[39] Bonel, G. 1972. Contribution a l'etude de la carbonation des apatites. Part I. Ann. Chim 7, 65-87.

[40] Thompson, D. D., W. S. Posner, A. N. C. Laughlin, and N. C. Blumenthal. 1983. Comparison of bone apatite in osteoporotic and normal eskimos. Tissue Int 35, 392-393.

[41] Pleshko, N., A. Boskey, and R. Mendelsohn. 1991. Novel infrared spectroscopic method for the determination of crystallinity of hydroxyapatite minerals. Biophys 60, 786–793

[42] Paschalis, E. P., F. Betts, R. Mendelsohn, and A. L. Boskey. 1996. Fourier transform infrared spectroscopy of the solution-mediated conversion of amorphous calcium phosphate to hydroxyapatite: new correlations between X-ray diffraction and infrared data. Calcif. Tissue 58, 9–16.

[43] Adele, L. and M. Richard. 2005. Infrared spectroscopic characterization of mineralized tissues. Vib Spectrosc 38, 107–114.

[44] Elisa, B., T. Paola, G. Massimo, G. Roberto, and B. Adriana. 2006. Nanocomposites of hydroxyapatite with aspartic acid and glutamic acid and their interaction with osteoblast-like cells Chair of Surgical Pathophysiology 25, 4428-4433.

[45] Stewart, S. D. A., C. P. Shea, M. D. Tarnowski, D. Morris, and R. Wang. 2002. Trends in early mineralization of murine calvarial osteoblastic cultures: a Raman microscopic study. Raman Spectrosc 33, 536–543.

[46] Raisz, L. G. 1992. Mechanisms and regulation of bone resorption of osteoclastic cells. Raven Press, 287-311.

[47] Bart, C. 2008. Normal Bone Anatomy and Physiology. Clin J Am Soc Nephrol. S131–S139.

[48] Jitomir, J. and D. S. Willoughby. 2008. Leucine for retention of lean mass on a hypocaloric diet. Leucine for retention of lean

mass on a hypocaloric diet. 11, 606-9.

[49] Yamaguchi, M. and R.Yamaguchi.1986. Action of zinc on bone metabolism in rats: Increase in alkaline phosphatase activity and DNA content. Biochem Pharmacol. 35, 773–777.

[50] Yamaguchi, M., H. Oishi, and Y. Suketa. 1987. Stimulatory effect of zinc on bone formation in tissue culture. Biochem Pharmacol. 36, 4007–4012.

[51] Yamaguchi, M., H. Oishi, and Y. Suketa.1988. Zinc stimulation of bone protein synthesis in tissue culture. Biochem Pharmacol. 37, 4075–4080.

[52] Saeed, H., N. Roghayeh, and N. Hamid, N. 2009. Physico–Chemical and In Vitro Biological Study of Zinc-Doped Calcium Sulfate. Wiley InterScience

[53] Moonga, B. S. and D. W. Dempster. 1995. Zinc is a potent inhibitor of osteoclastic bone resorption in vitro. Bone Miner Res. 10, 53–457

[54] Hashizume, M. and M. Yamaguchi. 1993. Stimulatory effect of beta-alanyl-L-histidinato zinc on cell proliferation is dependent on protein synthesis in osteoblastic MC3T3-E1 cells. Mol Cell Biochem. 122, 59–64.

[55] Hashizume, M. and M. Yamaguchi.1994. Effect of beta-alanyl-L-histidinato zinc on differentiation of osteoblastic MC3T3-E1 cells: increases in alkaline phosphatase activity and protein concentration. Mol Cell Biochem. 131, 19–24.

[56] Stein, G. S., J. B. Lian, and T. A. Owen. 1990. Relationship of cell growth to the regulation of tissue-specific gene expression during osteoblast differentiation. Faseb. 4, 3111–3123.

[57] Franceschi, R. T. and B. S. Iyer.1992. Relationship between collagen synthesis and expression of the osteoblast phenotype in MC3T3-E1 cells. Bone Miner Res. 7, 235–246.

[58] Coen, G., P. Ballanti, and E. Bonucci. 1998. Bone markers in the diagnosis of low turnover osteodystrophy in haemodialysis patients. Nephrol Dial Transplant. 13, 2294–302.

[59] Kamimura, H., N. K. O. Koga,H. Yoshimura,H. Inoue,K. Sato, and M. Ohkubo. 1989. Studies on distribution, excretion and subacute toxicity of squalene in dogs. Fukuoka Igaku Zasshi. 80, 269-280.

[60] Sandar , B. G. L., Z. M. Svetomir, I. Suzana, A. M. Dimitrijevi, andU. S. Dejan. 2007. Antimicrobial activity of the essential oil and differentfractions of juniperus communis l. and a comparison with some commercial antibiotics, Serbian Chemical Society. 72: 311-320.

[61] Lai, Y. L. and M.Yamaguchi. 2009. Phytocomponent p-hydroxycinnamic acid stimulates bone formation and inhibits bone resorption in rat femoral tissues in vitro. Mol Cell Biochem. 292, 45-52.

[62] Kotha, S. P., M. Lieberman, A. Vickers, S. R. Schmid, and J. J. Mason. 2006. Adhesion enhancement of steel fibers to acrylic bone cement through a silane coupling agent. J Biomed Mater Res A. 76, 111-9.

[63] Nikolaos, K. and T. Margaret. 2010. Spectroscopic assessment of normal cortical bone: Differences in relation to bone site and sex, Scientific World. 10: 402–412.

[64] Nyquist, R. A., C. L. Putzig, and M. A. Leugers. 1997. The handbook of infrared and raman spectra of inorganic compounds and organic salts Edited by: San Diego, USA: Academic Press.